Spectroscopic Observation and Characterization of H+H− Heavy Rydberg States[†]

M. O. Vieitez, T. I. Ivanov, E. Reinhold, C. A. de Lange, and W. Ubachs*

Laser Centre, Vrije Universiteit, Amsterdam, Netherlands

Received: April 30, 2009; Revised Manuscript Received: June 22, 2009

A series of discrete resonances was observed in the spectrum of H_2, which can be unambiguously assigned to bound quantum states in the $1/R$ Coulombic potential of the H+H− ion-pair system. Two-step laser excitation was performed, using tunable extreme ultraviolet radiation at $\lambda = 94-96$ nm in the first step, and tunable ultraviolet radiation in the range $\lambda = 310-350$ nm in the second step. The resonances, detected via H^+ and H_2^+ ions produced in the decay process, follow a sequence of principal quantum numbers ($n = 140-230$) associated with a Rydberg formula in which the Rydberg constant is mass scaled. The series converges upon the ionic H+H− dissociation threshold. This limit can be calculated without further assumptions from known ionization and dissociation energies in the hydrogen system and the electronegativity of the hydrogen atom. A possible excitation mechanism is discussed in terms of a complex resonance. Detailed measurements are performed to unravel and quantify the decay of the heavy Rydberg states into molecular H_2^+ ions, as well as into atomic fragments, both H($n = 2$) and H($n = 3$). Lifetimes are found to scale as n^3.

1. Introduction

The presence of ion-pair states and ionic binding in molecules has long been recognized. In diatomic molecules potential energy curves are known whose outer limb of the potential curve closely overlaps with the Coulombic $1/R$ attraction of the ionic constituents. Such electronic states were investigated in ICl[1] and in I_2.[2] Also, in H_2 molecular states were identified for which the outer limb follows the H+H− potential. In the low-energy region this holds for the well-known $EF^1\Sigma_g^+$ and the $B^1\Sigma_u^+$ states. At higher excitation energies, the $H\bar{H}^1\Sigma_g^+$ and the $B''\bar{B}^1\Sigma_u^+$ states were identified with dominant ionic character at large internuclear separation.[3,4] At even higher energies in the H_2 molecule additional electronic states of ion-pair character were predicted,[5,6] but experimental searches for bound levels are still inconclusive.[7]

The photoexcitation, and the photophysics including ionization and dissociation phenomena above the ion-pair threshold have been widely investigated over the years. Suits and Hepburn published a review on the spectroscopy and dynamics of ion-pair dissociation processes.[8] While many of the ion-pair phenomena have been observed in diatomic molecules (see, e.g., the work on Cl_2),[9−11] some of the studies have focused on polyatomics as well: the excitation mechanism of ion-pair states in bromomethane was recently investigated.[12] Previously, it had been demonstrated that ion-pair dissociation (in N_2O) can also lead to an unstable fragment (N−) which then autodetaches.[13]

The H_2 molecule is often chosen as the benchmark target for investigation of ion-pair phenomena in molecules. Already in the early studies involving classical light sources by Chupka et al.[14] and by McCulloh and Walker,[15] a strong coupling was found in the H+H− continuum above 17.3 eV between the ion-pair channel and electronic Rydberg series converging upon highly excited vibrational levels of H_2^+. In the ion-pair photoionization production curve (obtained via H− detection), the structure of predissociating and autoionizing Rydberg series was clearly observed. Pratt and co-workers applied a laser multistep excitation scheme to investigate the same energy

region in H_2;[16] they found strong coupling of the H+H− continuum to electronic Rydberg series converging upon $v^+ = 9$ in the H_2^+ ion. In a subsequent study[17] it was found that the observed resonances above the H+H− threshold decay via autoionization as well as dissociation involving H($n = 3$) and H($n = 4$) dissociation products. Kung and co-workers[18] approached the same energy region above the H+H− limit via intermediate states ($C^1\Pi_u$, $v' = 2$) and ($B^1\Sigma_u^+$, $v' = 12$) of ungerade symmetry. They observed the same Rydberg series converging to $v^+ = 9$ in the H_2^+ ion, again employing H− detection. This once more demonstrated the strong coupling between the H+H− ion-pair and the electronic Rydberg channels. This coupling is of importance for the effective oscillator strength for quantum states in the H+H− potential. The studies mentioned here were all focused on the energetic region above the ion-pair threshold.

The energy region very near and just below the onset of the H+H− threshold was investigated by various laser spectroscopic methods. Shiell et al. applied the threshold ion-pair production spectroscopy (TIPPS) technique to the H+H− system,[19] therewith demonstrating the existence of long-lived high-n ion-pair, or heavy Rydberg states. Reinhold and Ubachs provided further evidence for such high-n heavy Rydberg states by producing wave packets of angular momentum states in an electric field and following their time evolution before pulsed field dissociation (i.e., ion-pair formation).[20] The temporal behavior in the wave packet dynamics can be quantitatively interpreted in terms of a heavy Rydberg system, or a "heavy Bohr atom": a hydrogen atom, in which the negatively charged electron is exchanged for a composite H− particle, which is treated as a point-like entity.[21] It was postulated that heavy Rydberg systems follow the physical laws of electronic Rydberg systems and that each system can be described by a single mass-scaling parameter that defines all properties of heavy Rydberg states. This was tested and quantitatively demonstrated in detecting wave packet dynamics in the H+F− system,[22] which has a reduced mass differing by a factor of 2 from the H+H− system.

As a follow-up on a recent Letter on the observation of a spectrum of energy-resolved heavy Rydberg states in the

---

[†] Part of the "Robert W. Field Festschrift".
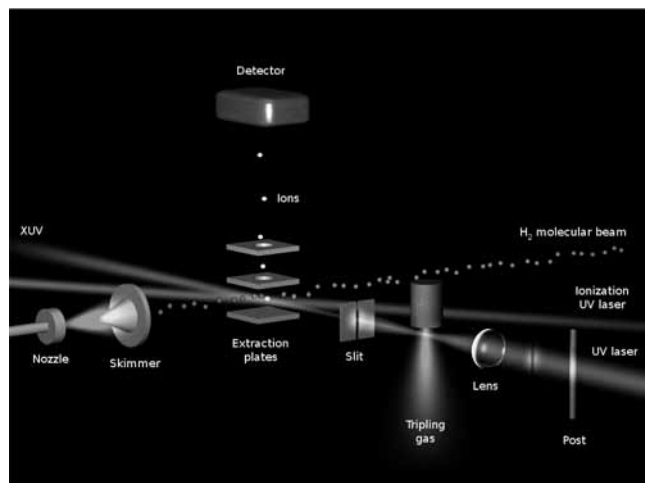* To whom correspondence should be addressed.

Figure 1. Experimental setup. An XUV laser beam, generated via third harmonic generation in a jet of krypton, intersects a molecular beam of H_2. Counter-propagating is a second UV laser beam, further exciting the H_2 to heavy Rydberg resonances. Ions (H_2^+ and H^+) produced after decay are accelerated by extraction field plates and detected after time-of-flight selection.

H^+H^- system[23] we here report on a fuller description of these remarkable features. Regularly structured resonances are detected that obey a generalized Rydberg formula[21]

$$E_n = E_{IP} - \frac{R_h}{(n - \delta)^2} \qquad (1)$$

with n the principal quantum number observed over the range $140 - 230$, E_{IP} the ion-pair threshold, R_h the Rydberg constant of the heavy system, and δ a quantum defect, which is usual for a nonpoint-like system.[24,25] Although the assignment of principal quantum numbers to the observed heavy Rydberg states is unambiguous, there still exist some open issues about the spectroscopic features. They concern the excitation mechanism of heavy Rydberg states, their quantum defects, and their interactions with electronic Rydberg states; these form the subject of the present paper.

2. Experiment and Observations

The range of excitation energies $134\,000 - 138\,000$ cm^{-1} in the H_2 molecule (above the $v'' = 0$, $J'' = 0$ ground state of *para*-H_2) is investigated via two-step laser excitation in an experimental configuration as schematically displayed in Figure 1. The first step is induced by tunable extreme ultraviolet (XUV) radiation, which is produced by third harmonic generation in a krypton gas jet. The XUV-laser is tuned and fixed at some intermediate resonances in H_2. Here any strong line in the spectrum of the Lyman and Werner absorption bands can be chosen; we performed the studies at XUV-wavelengths at which resonance-enhanced third harmonic (THG) in krypton can be utilized to deliver abundant amounts of XUV radiation. Such resonances are found to exist at $\lambda = 94.6$, 95.1, 95.25, and 96.3 nm.[26] At the wavelength positions of these THG resonances the low rotational states in the $B^1\Sigma_u^+ - X^1\Sigma_g^+$ (12,0) and $C^1\Pi_u - X^1\Sigma_g^+$ (3,0) bands can be probed. A special experimental feature in the present study is the filtering of the powerful fundamental radiation (used in the third harmonic generation process) from the XUV-harmonic by a method of spatially selective phase-matching as discussed in ref 27. This is done

to avoid nonresonant ionization of the excited H_2 molecule by the powerful UV pulses from the first laser.

In a second excitation step a tunable ultraviolet (UV) laser pulse in the range $310 - 355$ nm, obtained from a frequency-doubled pulsed dye laser, is employed to transfer the population of the intermediate states to the energetic region, where the heavy Rydberg states are expected. Pulses from both lasers are spatially overlapped in a region where they perpendicularly intersect a pulsed and skimmed molecular beam of pure H_2. Temporal overlap is also required in view of the short lifetimes of the intermediate states (≈ 0.5 ns). Signal is detected by either monitoring H_2^+ ions generated from immediate decay of the H^+H^- resonances or H^+ ions, produced via dissociation involving $H(n = 2)$ and $H(n = 3)$ products; the latter are subsequently ionized by the UV laser. Time-of-flight mass selection permits distinguishing signals from either H_2^+ or H^+ ions. Pulse extraction takes place after both laser pulses so that excitation of the heavy Rydberg states is warranted under field-free conditions.

In Figure 2 a spectral recording of a heavy Rydberg series is shown when using $B^1\Sigma_u^+$, $v' = 12$, $J' = 1$ in *para*-hydrogen as an intermediate state. The spectrum is calibrated to a total excitation energy (above $X^1\Sigma_g^+$, $v'' = 0$, $J'' = 0$ in the neutral H_2 molecule) by adding the calibration of the second tunable UV-laser to the level energies of the intermediate states. The R(0) line in the B-X(12,0) band is at 103844.62 cm^{-1},[28] hence this is also the level energy of the $B^1\Sigma_u^+$, $v' = 12$, $J' = 1$ intermediate state. This recording clearly shows the series of resonances that can be assigned to heavy Rydberg states of principal quantum numbers $n = 135 - 154$, indicated in Figure 2. In the region above 135500 cm^{-1} this series is interrupted and instead electronic Rydberg series appear that converge to $v^+ = 6$, $N^+ = 0$, 2, and 4 in H_2^+.

Figure 3 shows a second spectral recording of the heavy Rydberg series in *para*-H_2, now using the R(0) line in the C-X(3,0) band in the first excitation step. Hence the $C^1\Pi_u$, $v' = 3$, $J' = 1$ level of (-) or (e) parity at 105660.80 cm^{-1} above the H_2 ground state acts as the intermediate state. This spectrum clearly shows resonances that can be assigned as heavy Rydberg states with principal quantum numbers $n = 162 - 191$. In this spectrum no signatures of electronic Rydberg series are discernible, although electronic Rydberg series converging to $v^+ = 7$ are expected in this energy range.

In addition to the excitation spectra displayed in Figures 2 and 3, both obtained in *para*-hydrogen, also spectra in *ortho*-hydrogen were recorded. In such spectra, located in the energy range $135\,650 - 135\,880$ cm^{-1}, using the P(1) line in the B-X (12,0) band of H_2, heavy Rydberg series are observed as well; a recording is shown in Figure 3 of ref 23. In those observations excitation of the heavy Rydberg series competes with excitation of electronic Rydberg series converging to the $v^+ = 6$, $N^+ = 1$ and 3 limits in the H_2^+ ion.

An important experimental result when studying Rydberg series is a determination of quantum defects. Rearranging eq 1 yields an expression for an effective quantum defect:

$$\delta_n = n - \sqrt{\frac{R_h}{E_{IP} - E_n}} \qquad (2)$$

where E_n is an observed line position and n is the (integer) quantum number assigned to that particular resonance. Determination of quantum defects can be accomplished by fitting of the spectral line shapes. While in principle the quantum defect
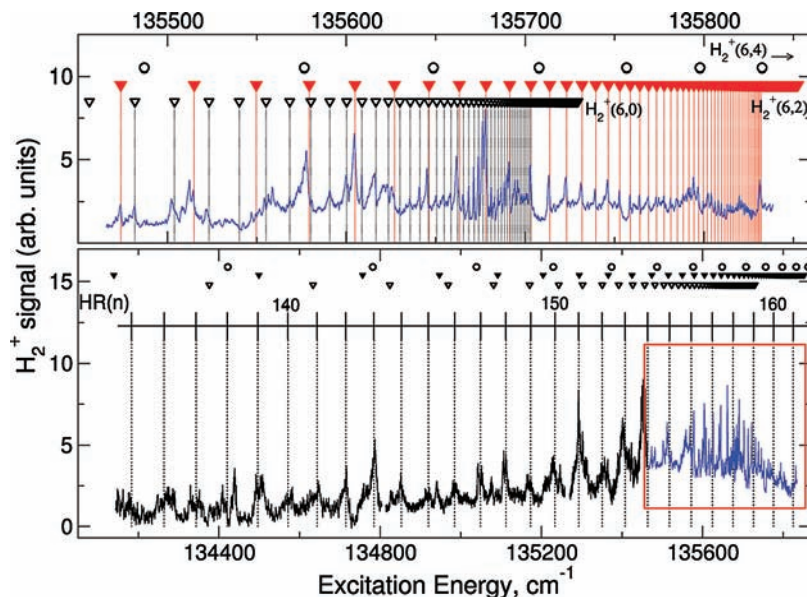
H+H− Heavy Rydberg States

J. Phys. Chem. A, Vol. 113, No. 47, 2009 **13239**

Figure 2. Lower panel: Characteristic spectrum after two-step laser excitation via B–X (12,0) R(0) in the *para*-H_2 molecule. The markers and dotted lines show the predicted positions of the heavy Rydberg series between $n = 134$ and $n = 161$. In the range between $n = 154$ and 161, the series is interrupted. In the upper panel, the part of the spectrum between 135 465 and 135 840 cm^{-1} is enlarged, showing in detail the corresponding resonances for the electronic Rydberg series converging to the H_2^+ ($v^+ = 6$, $N^+ = 0$, 2, and 4) states; these states are denoted with open triangles, full triangles, and open circles, respectively.
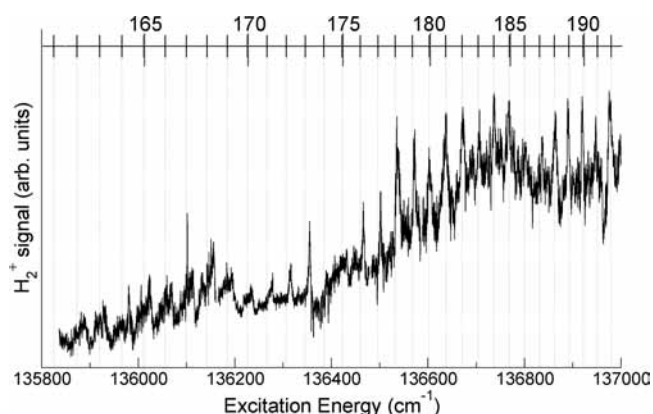

Figure 3. Spectrum obtained in two-step laser excitation via C–X (3,0) R(0) in the *para*-H_2 molecule. The markers and connected vertical lines show the predicted positions of the heavy Rydberg series between $n = 162$ and 192.

Figure 4. (a) Calculated quantum defects δ_n, from the complex resonance model, assuming the interlopers are the Rydberg states ($n = 5$–7) converging to H_2^+ ($v^+ = 9$) $N^+ = 0$ (marked with full lines), $N^+ = 2$ (marked with dashed lines), and $N^+ = 4$ (marked with dotted lines). The electronic Rydberg states are assumed to have zero quantum defect. (b) Observed quantum defects δ_n obtained from spectra of *para*-hydrogen, using two different intermediate states: $B^1\Sigma_u^+$, $v' = 12$, $J' = 1$ and $C^1\Pi_u$, $v' = 3$, $J' = 1$.

can be larger than 1 in a system with an extended core (as for the *s*-series in alkali atoms), here only the fractional part of the quantum defect δ_n is deduced. Problems in determining the values for δ_n lie in the treatment of the structured underlying continuum that gives rise to background slopes, in the moderate signal-to-noise ratio, and in the occurrence of asymmetric Fano-type line profiles. These phenomena lead to uncertainties in the determination of the quantum defects. Analysis of the spectra obtained for *para*-hydrogen, for which long series of heavy Rydberg states are observed, results in values of quantum defects as plotted in the lower panel of Figure 4.

Another feature associated with the heavy Rydberg resonances is their width as observed in the spectral recordings. In many cases asymmetric line shapes were observed, and in other cases the underlying continuum was very structured, making it difficult to derive a reliable value for the resonance width. For those transitions observed at reasonable signal-to-noise ratio and with a symmetric line profile the widths Γ were determined and plotted in Figure 5.

The spectra displayed in Figures 2 and 3 are recorded by monitoring H_2^+ signal. Indeed, autoionization is the most
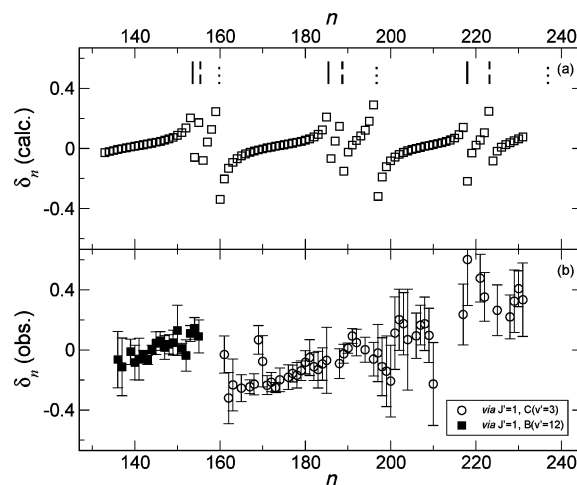
significant decay channel, forming H_2^+ ions in all quantum states below the total excitation energy, i.e., $v^+ = 0$–5. Detection of H_2^+ is a means of recording the heavy Rydberg states, although in the present study we cannot determine the final ionic states H_2^+ (v^+, N^+). A competing channel (difficult to quantify but we estimate several 10%) is photodissociation in which the heavy Rydberg states decay into H($n = 1$) + H($n = 2$) and into H($n = 1$) + H($n = 3$). The second UV-laser exciting the heavy Rydberg states further ionizes both H($n = 2$) and H($n = 3$), producing H^+ that can be detected separately from H_2^+ in the time-of-flight setup. To further distinguish and characterize the dissociation channels the ion particle detector was replaced by a velocity map ion-imaging setup[29] to investigate if both dissociation pathways indeed occur. A result recorded upon
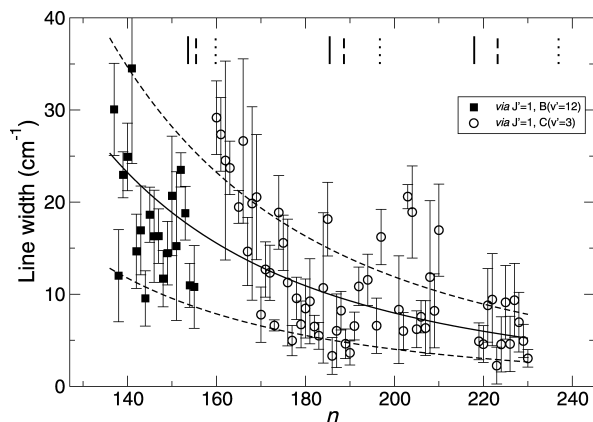
Figure 5. Linewidths Γ for some of the heavy Rydberg resonances observed with good signal-to-noise ratio and symmetric line shapes as a function of principal quantum number n. The central (full) line represents a fit to a functional form $\Gamma \propto n^{-3}$ with the outer (dashed) curves representing the 1σ uncertainty.
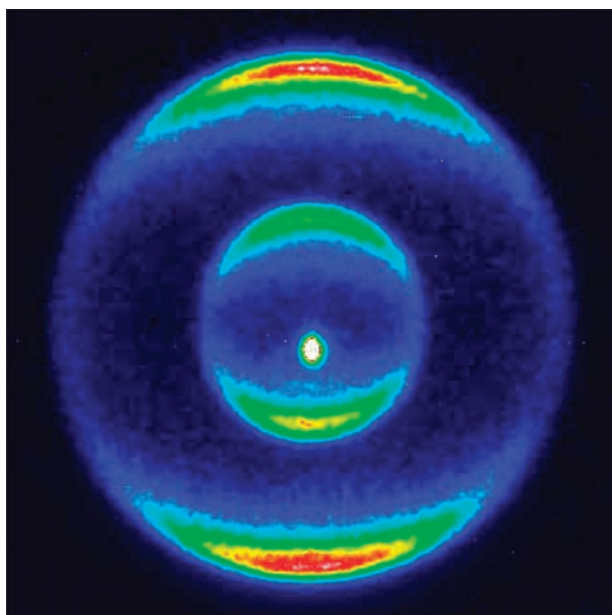

Figure 6. Ion image representation of the kinetic energy distribution upon excitation of a heavy Rydberg resonance. The XUV beam passes from left to right, the second UV laser beam from right to left; polarizations are linear and parallel and in the plane of the paper. The outer ring corresponds to H^+ ions of high kinetic energy in decay to a $H(n = 2)$ fragment, whereas the inner ring represents decay to $H(n = 3)$. The off-center dot represents detection of H_2^+ ions; the offset from the center is related to the fact that H_2^+ are accelerated to lower velocities in a typical velocity-map-imaging configuration than H^+. Therefore they travel a longer time along the direction of the molecular beam, which is from up to down in the figure. Note that we present raw data here, which are not 2D → 3D inverted.

excitation of the $n = 191$ heavy Rydberg resonance at 136950 cm^{-1} excited via the $C^1\Pi_u$, $v' = 3$ intermediate state is shown in Figure 6. This experiment indeed proves that both $H(n = 2)$ and $H(n = 3)$ are produced. The ring structures can be unambiguously assigned to the kinetic energies required for these channels. In the outer ring $H(n = 2)$ atoms are detected that have higher kinetic energy from the dissociation process. In the inner ring the $H(n = 3)$ atoms, that have higher internal energy and lower kinetic energy, are probed. No distinction is made between 2s and 2p atoms, or between 3s, 3p, and 3d hydrogen atoms. The angular distributions can be interpreted

to gain further understanding of the decay mechanism; this is outside the scope of the present work, but will be pursued in the future.[30]

3. Analysis

3.1. Interpretation of Observed Features. In the spectra two distinct phenomena are apparent. First, series of electronic Rydberg series are observed. From an intermediate state with a 2p electron, $2p\sigma$ in case of the $B^1\Sigma_u^+$ state and $2p\pi$ in case of $C^1\Pi_u$, ns and nd series can be expected. Due to selection rules Rydberg series in *ortho*-H_2 can converge upon $N^+ = 1$ and 3, and series in *para*-H_2 upon $N^+ = 0$, 2, and 4 for each v^+ vibrational quantum number.[31] The (v^+, N^+) ionization limits can be calculated from the value of the ionization energy of H_2 (124 417.48 cm^{-1})[32] and the level energies in the H_2^+ ion.[33]

In the spectrum of Figure 2, excited via the $B^1\Sigma_u^+$, $v' = 12$, $J' = 1$ intermediate state in *para*-H_2, three series are observed, converging to $v^+ = 6$, $N^+ = 0$, 2, and 4 states in the H_2^+ ion. These states show the typical behavior of series interaction as often observed in electronic Rydberg series in the H_2[31,34] and HD[35] molecules. One of the visible effects of interaction of a series with continua is that the Rydberg states converging upon the $v^+ = 6$, $N^+ = 4$ limit clearly appear as window resonances in Figure 2. It is noted that it requires an nd Rydberg series converging upon $N^+ = 4$ to be observed in excitation from an intermediate state of total angular momentum $J' = 1$; selection rules do not permit excitation of an ns series converging to $N^+ = 4$. Similar electronic Rydberg series were observed in excitation via the $B^1\Sigma_u^+$, $v' = 12$, $J' = 0$ state in *ortho*-H_2. Selection rules impose that only Rydberg states converging to $v^+ = 6$, $N^+ = 1$ and 3 should be observable, which is indeed the case. Again, qualitatively some features of series interaction are visible in the spectrum of Figure 3 in ref 23. In the Rydberg series converging to $v^+ = 6$, $N^+ = 3$ the Fano q-parameter is found to vary as a function of the principal quantum number, indicative of an interaction between multiple channels. However, the observations on electronic Rydberg states are not the predominant issue in the present study, and are left for future analysis.

The second and key feature in the spectra is the observed series of broad resonances that follows eq 1, the heavy Rydberg series, as indicated in the spectra of Figure 2 and 3 for *para*-H_2, and in Figure 3 of ref 23 for *ortho*-H_2. They represent the first spectroscopic observation (i.e., frequency-domain resolved resonances) of heavy Rydberg states in a molecular system. The assignment in terms of heavy Rydberg states is unambiguous, since the spectral features follow the representation by eq 1 without invoking adjustable parameters. As discussed by Reinhold and Ubachs[21] the crucial parameters can be calculated in elementary fashion. The Rydberg constant R_h for the H^+H^- heavy Bohr atom can be obtained by replacing the electron by an H^- particle, yielding the scaling factor $(\mu/m_e) = 918.5761$. Hence, via $R_h = (\mu/m_e)R_\infty$, one obtains: $R_h = 1.00802 \times 10^8$ cm^{-1}. The other parameter in eq 1, the value for the ion-pair dissociation limit E_{IP}, can be determined from $E_{IP} = IE(H_2) + D_0(H_2^+) - EA(H)$, yielding $E_{IP} = 139\ 713.83\ cm^{-1}$. Based on these parameters, and choosing zero quantum defects ($\delta_n = 0$), the positions $HR(n)$ of the heavy Rydberg states in Figures 2 and 3 can be calculated in a straightforward manner. The positions of zero quantum defects are indicated in the figures with dotted lines to guide the eye. The observed resonances clearly follow the calculated regular structure of the heavy Rydberg states, making the assignment unambiguous.

3.2. On Quantum Defects. There are some striking observations in the spectra, which require further discussion and
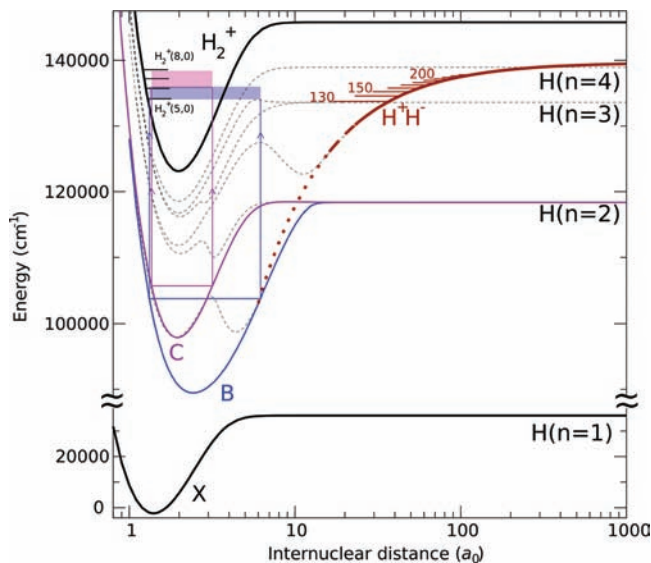
H$^+$H$^-$ Heavy Rydberg States

J. Phys. Chem. A, Vol. 113, No. 47, 2009 **13241**

Figure 7. Potential-energy diagram of the H$_2$ molecule with distinction between two separated regimes: for $R < 12a_0$ the range of internuclear distances where covalently bound states and the electronic Rydberg states converging upon H$_2^+(v^+, N^+)$ dominate (dashed lines representing the potential curves of *gerade* symmetry in this region),[3-7] and the range $R > 12a_0$ where H$^+$H$^-$ heavy Rydberg states exist. The H$^+$H$^-$ Coulomb potential is shown in dark (red) and extended to smaller R by dots. Intermediate energy levels in the B and C states (at $\sim$105 000 cm^{-1} excitation) are indicated and their accessible Franck–Condon ranges mapped (boxes).

explanation. Here we address three: the fact that the heavy Rydberg states are only observed for principal quantum numbers $n > 100$, the issue of angular momentum quantum numbers and selection rules, and the question as to where the oscillator strength for exciting heavy Rydberg states originates.

Effective quantum defects for the heavy Rydberg series are derived and plotted in Figure 4. The Bohr radius in a two-particle quantum system is defined by[21]

$$a_0 = \frac{4\pi\varepsilon_0\hbar^2}{\mu e^2} \tag{3}$$

with μ the reduced mass of the heavy Bohr system (918.5761 m_e). Hence, the Bohr radius a_0^h of the heavy Bohr system (H$^+$H$^-$) becomes as small as 5.76×10^{-14} m. This is much smaller than the extension of the composite H$^-$ particle;[36] consequently, the model of heavy Rydberg states breaks down at small internuclear separation, or at small principal quantum numbers n. The potential energy diagram (Figure 7) shows how the H$^+$H$^-$ Coulombic $1/R$ potential is affected by perturbations of covalent states even at large internuclear separation. Near the H($n = 2$) dissociation threshold there is a large interaction, with an avoided crossing of some 3000 cm^{-1} at $\approx 10a_0$. If the H$^+$H$^-$ potential can be considered pure for $R > 12a_0$, this means $R = n^2a_0^h \approx 12a_0 \approx 6 \times 10^{-10}$ m, and the description in terms of heavy Rydberg states may be considered valid only above $n \approx 100$. It is noted that perturbations with covalent states exist at internuclear separations of $36a_0$ and at some $250a_0$, where the H($n = 3$) and ($n = 4$) dissociation curves cross.[5-7] These perturbations are much weaker, but should be included in more refined models of H$^+$H$^-$ heavy Rydberg states. The above considerations imply that quantum defects in the heavy Bohr system are large, much larger than in the *s*-series of alkali atomic systems. Pan and Mies[24] have calculated such quantum defects

for the Li$^+$I$^-$ ionically bound system from first principles, and deduced that the lowest 177 angular momentum states are removed from the purely Coulombic spectrum. Previously Asaro and Dalgarno had found a number of 128 excluded levels in the Li$^+$F$^-$ system.[37] In the experimental analysis we will deal, as usual, with the fractional part of the quantum defects δ_n.

In the work of Pan and Mies[24] a relation was also established between sets of quantum numbers as commonly used for Rydberg states (n, l, m) and those usually invoked to describe molecular motion (v, J, M). The orbital angular momentum is described as l equivalent to J, with projections of a magnetic quantum number m or M. A connection for the principal quantum number can be established through the relation $n \leftrightarrow v + J + 1$. Hence, the equation for the Rydberg energy levels can be written as:[24]

$$E_{v,J} = E_{IP} - \frac{R_h}{(v + J + 1 - \delta_J)^2} \tag{4}$$

where the J-dependence of the quantum defect is explicitly written. In most of the spectra reported here, H$_2$ is excited in its *para*-configuration via a R(0) transition in the first step. Hence, from the intermediate $J' = 1$ state, following the $\Delta l = \Delta J = \pm 1$ selection rule, in principle two heavy Rydberg series can be excited, with $J = 0$ and $J = 2$ angular momenta. These series may possess different quantum defects δ_0 and δ_2, since low angular momentum states are known to exhibit strongly varying quantum defects; an example is the strong difference between the s and p electronic Rydberg series in the Na atom. In our experiments we only observe a single heavy Rydberg series for *para*-H$_2$. Clearly, this requires an explanation.

Notably, Pan and Mies[24] have shown in a theoretical analysis of the Li$^+$ I$^-$ heavy Rydberg system, that for the low angular momentum states the quantum defects δ_J can vary as by much as 1 for each step in J. If such a situation would also prevail in the *para*-H$^+$H$^-$ system, the two heavy Rydberg series that are expected would approximately coincide. The same would be true if both quantum defects δ_0 and δ_2 would differ by zero or any integer number. Without any knowledge about quantum defects, an explanation for the observation of only a single series must remain tentative. In *ortho*-H$_2$, when using the P(1) transition in the first step to excite the molecule from X$^1\Sigma_g^+$, $v'' = 0$, $J'' = 1$ to a $J' = 0$ intermediate state, only a single heavy Rydberg state with $J = 1$ is expected and observed.

It is important to note that the heavy Rydberg series in both *para*- and *ortho*-H$_2$ possess the same ion-pair dissociation limit. This is not necessarily true for every heavy Rydberg series but is a consequence of the fact that both the H$^+$ and H$^-$ fragments possess no internal electronic structure. In addition, the distinction between *para*- and *ortho*-H$_2$ remains unaffected even if the nuclear spins have an internuclear separation of $\approx 12a_0$ or more (several hundred a_0 in case of $n = 200$). This once more underlines the fact that it is not the distance-dependent interaction between the nuclear spins, but only the different symmetries of the nuclear spin wave functions that cause the *ortho-para* distinction. Another point of interest concerns the fact that situations in which both electrons are positioned on either nucleus A or B should be indistinguishable. If we define the corresponding 'localized' wave functions as A and B, the true degenerate solutions of the Schrödinger equation are $^1/_{\sqrt{2}}(\Psi_A \pm \Psi_B)$. However, even very small stray electric fields will lift this degeneracy due to the large polarizability of heavy Rydberg states.[21]

3.3. Intensities via Channel Interaction: Complex Resonance. The mechanism for exciting molecular ion-pair states has been discussed in the literature[2,12] and Franck−Condon arguments play a role. High-n states in H^+H^- cannot be directly excited from the intermediate states $B^1\Sigma_u^+$, $\nu' = 12$ and $C^1\Pi_u$, $\nu' = 3$, because their wave function density is confined to $R < 6a_0$ and $R < 3a_0$, respectively. The internuclear distances at which the intermediate states exhibit wave function density is mapped onto the energy region of the heavy Rydberg states with color-(gray) shaded rectangles in Figure 7. Intensities I_n for excitation of heavy Rydberg states, based on Franck−Condon factors, should follow

$$I_n = |\int \Psi_n^*(R)\Psi_{B,C}(R)\, dR|^2 \qquad (5)$$

Similar to usual Rydberg wave functions of high principal quantum number, heavy Rydberg states exhibit a wave function with their density entirely located at large separation from the core, in this case the H^+H^- separation. In the language of molecular structure, the wave function is concentrated at the outer turning point of the H^+H^- potential. Inspection of Figure 7 indicates that this is at $R \approx 50 - 100a_0$. This implies that direct excitation of the heavy Rydberg states should be Franck−Condon forbidden. In order to provide an explanation for their excitation, the model of a complex resonance is invoked.

The observation of Rydberg series to which a direct transition is highly improbable has been reported for the atomic case.[38] For the molecular case this phenomenon was observed and analyzed for the case of H_2. Jungen and Raoult[39] developed a model of channel interaction that explains how a Rydberg series with zero transition dipole moment can borrow effective oscillator strength, which they baptized as a complex resonance. Later this phenomenon was modeled in basic form by Giusti-Suzor and Lefebvre-Brion.[40] Before giving details we consider if simpler models might explain the observed features; interaction between a heavy Rydberg series (without oscillator strength) with a broad continuum (which exhibits oscillator strength) would in a Fano-type analysis lead to window resonances, contrary to what is observed.

The complex resonance model involves (at least) three channels: one open channel represented by an ionization continuum, and two closed channels, viz. an interloper (i.e., a strong resonance, excited with a large transition dipole moment) and a (Rydberg) series of close-lying states. Couplings are assumed between each of the closed channels with the continuum, and between both closed channels. From this simple model it is shown that an interference takes place between on the one hand the direct interaction between both closed channels, and on the other hand the indirect interaction between the closed channels via the continuum. This interference effect can enhance or diminish the intensities of the observed transitions to both interloper and members of the Rydberg series, and also affects line positions, line shapes and widths. In general, an essential feature of the model is that any channel i, for which the transition dipole moment D_i is zero, can obtain an effective oscillator strength σ_i due to interference, such that it can be excited and observed.

In our case, the simple model of three interacting channels as presented in ref 40 is not exactly valid, but can easily be extended to a situation that involves more than one interloper. In a five-channel description, graphically displayed in Figure 8, we assume that the closed bound H^+H^- heavy Rydberg series
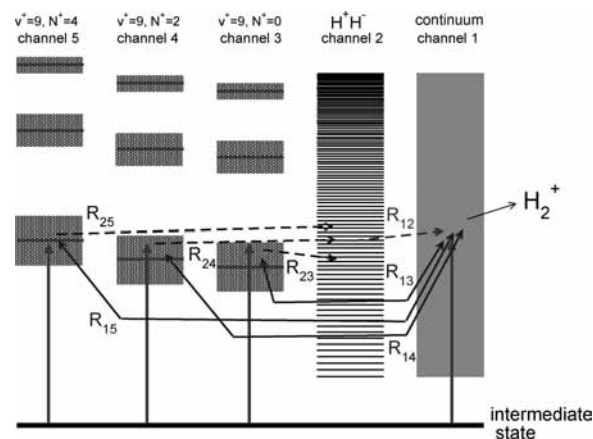

Figure 8. Interaction diagram for the model of a complex resonance in the case of the H^+H^- series. The interloper states are assumed to be members of the electronic Rydberg series converging upon the $H_2^+(\nu^+ = 9, N^+ = 0, 2,$ and 4) states of the ion (for the case of *para*-hydrogen; in case of *ortho*-hydrogen $N^+ = 1$ and 3). The upward pointing arrows represent transition dipole moments giving rise to direct excitation, while the sideways pointing arrows refer to channel interactions. Note that in this 5-channel model the electronic Rydberg series converging to $\nu^+ = 6$, as observed in the spectrum of Figure 2 are excluded; this is one of the many assumptions made.

(channel 2) possesses a zero transition dipole moment ($D_2 = 0$). A further simplification of this model is that interactions with the electronic Rydberg series as observed in Figures 2 are left out.

As far as interlopers are concerned, they are assumed to be low-n members of electronic Rydberg series that converge upon high ν^+ levels in the H_2^+ ion. From the work of Chupka et al.,[14] McCulloh and Walker,[15] Pratt and co-workers,[16,17] and Kung et al.[18] a strong coupling between the H^+H^- continuum and the H_2^+ ($\nu^+ = 9$) electronic Rydberg series is apparent. Therefore we hypothesize that our interloper states are members of this particular $\nu^+ = 9$ Rydberg series. Taking the oscillator strength to be continuous across the ion-pair dissociation limit, we assume that this coupling persists below the threshold.

Following angular momentum selection rules, from a p intermediate state ns and nd electronic Rydberg states can be excited. In view of the fact that p−nd transition dipole moments are larger than those for p−ns, we limit ourselves to nd states. In a Hund's case (d) coupling scheme for *para*-hydrogen nd electronic Rydberg series can converge upon three different limits ($N^+ = 0, 2,$ and 4) of the ionic ground state. Low-n members of these series will act as interloper states and will be denoted by the closed channels 3−5 in Figure 8, respectively.

As for the open continuum channel, at an excitation energy of 137 000 cm^{-1} the system is above the $\nu^+ = 5$ level of the ion. Hence, all the electronic Rydberg states converging upon the $\nu^+ = 0-5$ levels can contribute via autoionization to a background continuum signal of H_2^+. We consider only a single continuum as channel 1 in our model. This is another crude approximation of the true situation at hand.

Following a multichannel quantum defect theory (MQDT) approach similar to ref.,[40] we introduce a set of five adjusted channel wave functions, including an open channel (the interacting continuum, φ_1) and four closed channels: the H^+H^- series (φ_2) and three electronic Rydberg (interloper) series converging to $\nu^+ = 9$, $N^+ = 0, 2,$ and 4 (φ_3, φ_4, and φ_5, respectively). The total wave function of the system can be written as

H⁺H⁻ Heavy Rydberg States

J. Phys. Chem. A, Vol. 113, No. 47, 2009 **13243**

$$\psi = \sum_{i=1}^{5} Z_i \cos[\pi(\nu_i + \mu_i)]\varphi_i \qquad (6)$$

with Z_i the amplitudes, $\nu_1 = -\tau$ the open channel phase, and for $i = 2$

$$\nu_2 = \left(\frac{R_h}{E_{IP} - E}\right)^{1/2} \qquad (7)$$

the phase of the H⁺H⁻ series, where R_h is the Rydberg constant for the heavy Bohr atom (100 802 075 cm⁻¹) and E_{IP} is the ion-pair dissociation limit (139 713.83 cm⁻¹).[21] For the three interloper channels $i = 3-5$

$$\nu_i = \left(\frac{R_e}{E_{lim}^i - E}\right)^{1/2} \qquad (8)$$

and R_e is the Rydberg constant for the electronic Rydberg system $R_e = \mu(H_2^+ + e^-)/m_e$ (109 704.3945 cm⁻¹), and E_{lim}^i is the ionization limit of channel i, calculated using the values of ref 33 ($E_{lim}^3 = 139\,831.09$ cm⁻¹, $E_{lim}^4 = 139\,930.14$ cm⁻¹, and $E_{lim}^5 = 140\,157.49$ cm⁻¹). The effective quantum defects μ_i have been all set to zero. Note that in this 5-channel model we assume that the three interloper states do not mutually interact, and the observed electronic Rydberg series converging to $\nu^+ = 6$ are not included.

Similar as in ref 40, where a calculation was performed for the quantum defects of an electronic Rydberg series interacting with an interloper, we derive for the quantum defects of the heavy Rydberg series (channel 2):

$$\tan(x_2) = R_{23}^2 \cot(x_3) + R_{24}^2 \cot(x_4) + R_{25}^2 \cot(x_5) \qquad (9)$$

where $x_i = \pi(\nu_i + \mu_i)$ is the notation for the quantum defects and R_{ij} are the R-matrix elements representing the channel interactions. This is an important result: the resonance peaks will be found at the energies where this equation is fulfilled. The strength of the interaction between the interlopers and the H⁺H⁻ series (R_{23}, R_{24}, and R_{25} in our notation), as well as the exact location of the interloper states greatly affect the position of the observed H⁺H⁻ lines. This will be reflected in the values for the quantum defects δ_n of the H⁺H⁻ series. These values are calculated, assuming zero quantum defects (μ_i) for the interloper states converging to H_2^+ ($\nu^+ = 9$, $N^+ = 0$, 2, and 4).

We have attempted to reconstruct the findings on the experimental quantum defects from this model; the small amount of experimental information and the large error bars on the one hand, and the large number of parameters on the other hand do not allow for a fit or a one-to-one correspondence of the model. However, by scanning the parameter space the solution of $R_{23}^2 = 0.01\pi$, $R_{24}^2 = 0.01\pi$, and $R_{25}^2 = 0.03\pi$ somewhat mimics the observed trend in the observed quantum defects, as is displayed in Figure 4. This merely serves as an illustration on how the complex resonance model might explain trends in observed quantum defects of the heavy Rydberg series. By comparing Figures 4 and 5 it may be verified that at the locations of the interactions also resonances in the observed lifetimes seem to occur.

In view of all the assumptions made and the limited amount of spectroscopic information, we cannot provide a conclusive

model to quantitatively reproduce the entire spectrum of heavy Rydberg resonances, and the electronic Rydberg series observed in the same energy region. We have presented a general framework that gives some insight in the variation of the quantum defects as in Figure 4. Furthermore from the generalized model of ref 40 several conclusions relevant for our purpose can be drawn. Whereas in the previous investigations of complex resonances[39,40] the model was applied to electronic Rydberg series, here it describes properties of heavy Rydberg series: (i) Even if the members of a Rydberg series cannot be optically excited directly, coupling to an interloper and a continuum can still lead to their observation; (ii) The spectral range covered by a complex resonance can be much larger than the interloper width; (iii) The interaction strength between the Rydberg series and the interloper is of great importance, since it affects the widths and positions of the peak maxima of the series; (iv) Decay of the Rydberg resonances can occur into various channels including the continua. The latter is the subject of the next section.

3.4. Resonance Widths and Decay. The heavy Rydberg series are observed as short-lived resonances having typical widths of some 5−25 cm⁻¹, corresponding to a lifetime of a picosecond or even a fraction thereof. The observed linewidths are displayed in Figure 5 as a function of principal quantum number. The uncertainties in the data points are large, due to limited signal-to-noise ratio and asymmetries in the line shapes, but nevertheless some interesting conclusions can be drawn from these observations.

Lifetimes of Rydberg states are known to scale as $\tau \propto n^3$.[25] This is reflected in the observed scaling of the linewidths of Figure 5 as n^{-3}. Notwithstanding the large error margins the data in Figure 5 somewhat follow the expected scaling law. In addition there is at least indication of an increased line width near $n = 163$. This resonance may hint at the location of the effective interloper. If this is true the interferences in the multichannel problem give rise to enhanced widths, where in principle the complex resonance model allows for both the possibility of enhancement or reduction of the line width.

At $n \approx 200$ a line width of $\Gamma(200) = 10$ cm⁻¹ is observed. Following the usual n^3 dependence for Rydberg states, this would scale to $\Gamma(2000) = 0.01$ cm⁻¹, which would correspond to a lifetime of 0.5 ns. However, in the studies on heavy Rydberg wave packets[21] for $n = 2000$ a lifetime of 90 ns was actually observed, deviating by over 2 orders of magnitude from the n^{-3}-scaling based on lower n-values. In addition, for these higher-lying heavy Rydberg states decay into the H($n = 4$) dissociation channel was observed;[21] this was accomplished by selectively ionizing the H($n = 4$) fragments by laser pulses of 1064 nm. The presently observed heavy Rydberg states of $n < 230$ are below the H($n = 4$) dissociation threshold and therefore this decay channel is closed. Nevertheless, the lifetimes in the range $n = 130 - 230$ are much shorter than those in the higher energy region probed in the wave packet experiments.

This discrepancy may be resolved by considering the fact that the wave packet experiments were conducted in electric fields.[20,21] As is extensively discussed in the literature on zero-kinetic energy (ZEKE) spectroscopy[41,42] high-n Rydberg states are known to exhibit longer lifetimes in the presence of electric fields. Heavy Rydberg states have a large polarizability; even in small stray electric fields of <0.1 V/cm at high n values full l-mixing (or rather J mixing) occurs.[21] In the oscillatory motion of the angular wave packets population is transferred to high angular momentum states of the heavy Rydberg system. This gives rise to longer lifetimes than expected from n^3 scaling.

Indeed, as shown in Figure 11 of ref 21, lifetimes were found to scale as n^4, a clear indication of angular momentum mixing in the electric field.

3.5. Heavy Rydberg States in Other Systems. Heavy Rydberg states are expected to exist in other molecular systems and a viable question is whether the presently observed rather short lifetimes are typical for heavy Rydberg states, or whether they depend on the specifics of the level structure and associated decay channels of the H_2 molecule. In H_2 heavy Rydberg states can be observed in the range where vibrational autoionization occurs (into $v^+ = 0 - 5$ vibrational levels) and dissociation into channels with H($n = 2$) and H($n = 3$); this may seem an unfortunate situation giving rise to strong decay and broad resonances. Experimentally H_2 is the only system where frequency-resolved heavy Rydberg series are observed. During the course of the investigations it was attempted to register similar heavy Rydberg series in D_2, however unsuccessfully: only electronic Rydberg series were observed in the D_2^+ and D^+ signal channels. This absence might be attributed to the lack of a suitably located interloper state in D_2.

Stark wave packets were observed in both H^+H^- and in the H^+F^- system. In the latter system lifetimes of typically an order of magnitude larger were found[22] in the high n region where l-mixing is important. Hence, the $H^+ F^-$ system might be a candidate for observing frequency resolved heavy Rydberg series. We note that the Rydberg constant for heavy Rydberg series scales with μ/m_e, where μ is the reduced mass of the molecule. Therefore, for all systems heavier than H_2 the density of states for heavy Rydberg states increases, and it will be more difficult to observe them, in particular if the lifetimes are as short as in H^+H^-. Further it is noted that in polyatomic systems there is a multitude of series limits for heavy Rydberg states. Each bound quantum state (rovibrational, spin−orbit) in the positively or negatively charged ion-pair fragments provides such a limit. This will further enhance the density of heavy Rydberg states. Finally we note that the $p\bar{p}$ protonium system, consisting of a proton electromagnetically bound to an antiproton should exhibit a series of quantum states of the same density and spacing as in the H^+H^- system, since the Rydberg constants of those systems are similar. Experiments for detecting and investigating protonium are under way.[43,44]

4. Conclusion

The first spectroscopic observation of frequency-resolved heavy Rydberg states in a molecular system is reported. Bound quantum states in the $1/R$ potential in H^+H^- are detected for principal quantum numbers in the range $140-230$, as predicted from a generalized Rydberg formula, which is mass-scaled for the orbital motion of the H^- particle replacing the electron. The resonances decay via autoionization forming H_2^+ ions as well as via dissociation forming H($n = 3$) and H($n = 2$) products. Lifetimes scale with n^3 and are typically shorter than 1 ps for the quantum states investigated ($n = 140 - 230$). A complex resonance model is invoked, reproducing the observed quantum defects, and explaining the origin of the effective oscillator strengths of the heavy Rydberg series. In H^+H^- the series could be observed in excitation from states of $^1\Sigma_u^+$ and of $^1\Pi_u$ symmetry, and both in *para-* and *ortho-*hydrogen. Such heavy Rydberg resonances are hypothesized to exist in all A^+B^- diatomic molecules, as well as in polyatomic molecules.

References and Notes

(1) Wang, S.; Lawley, K. P.; Ridley, T.; Donovan, R. J. Field induced ion-pair formation from ICl studied by optical triple resonance. *Faraday Discuss.* **2000**, *115*, 345–354.

(2) Ridley, T.; de Vries, M.; Lawley, K. P.; Wang, S.; Donovan, R. J. The field-ionization of near-dissociation ion-pair states of I_2. *J. Chem. Phys.* **2002**, *117*, 7117–7121.

(3) Reinhold, E.; Hogervorst, W.; Ubachs, W.; Wolniewicz, L. Experimental and theoretical investigation of the $H\bar{H}^1\Sigma_g^+$ state in H_2, D_2 and HD and the $B''\bar{B}^1\Sigma_u^+$ state in HD. *Phys. Rev. A* **1999**, *60*, 1258–1270.

(4) de Lange, A.; Hogervorst, W.; Ubachs, W.; Wolniewicz, L. Double-well states of ungerade symmetry in H_2; first observation and *ab initio* calculation. *Phys. Rev. Lett.* **2001**, *86*, 2988–2991.

(5) Detmer, T.; Schmelcher, P.; Cederbaum, L. S. *Ab initio* calculations with a nonspherical Gaussian basis set: Excited states of the hydrogen molecule. *J. Chem. Phys.* **1998**, *109*, 9694–9700.

(6) Staszewska, G.; Wolniewicz, L. Adiabatic Energies of Excited $^1\Sigma_u$ States of the Hydrogen Molecule. *J. Mol. Spectrosc.* **2002**, *212*, 208–212.

(7) Koelemeij, J. C. J.; de Lange, A.; Ubachs, W. Search for outer-well states above the ionization potential in H_2. *Chem. Phys.* **2003**, *287*, 349–354.

(8) Suits, A. G.; Hepburn, J. W. Ion-Pair dissociation: spectroscopy and dynamics. *Annu. Rev. Phys. Chem.* **2006**, *57*, 431–465.

(9) Ishiwata, T.; Shinzawa, T.; Si, J. H.; Obi, K.; Tanaka, I. Optical-Optical Double-Resonance Spectroscopy of Cl_2: Analyses of the $0_u^+1_u$, and $2_u(^3P_2)$ Ion-Pair States. *J. Mol. Spectrosc.* **1994**, *166*, 321–337.

(10) Zhou, C.; Hao, Y.; Mo, Y. Ion-Pair Dissociation Dynamics of Cl_2: Adiabatic State Correlation. *J. Phys. Chem. A* **1996**, *261*, 175–180.

(11) Ishiwata, T.; Kasai, Y.; Obi, K. Observation of the $0_u(^3P_1)$ ion-pair state of Cl_2 by perturbation-facilitated optical-optical double resonance. *Chem. Phys. Lett.* **2008**, *112*, 8263–8272.

(12) Ridley, T.; Hennessy, J. T.; Donovan, R. J.; Lawley, K. P.; Wang, S.; Brint, P.; Lane, E. Evidence for Rydberg doorway states in photoion pair formation in bromomethane. *J. Phys. Chem. A* **2008**, *112*, 7170–7176.

(13) Hikosaka, Y.; Eland, J. H. D. Ion Pair dissociation from N_2O followed by autodetachment of $N^-(^1D_g)$. *Chem. Phys. Lett.* **2001**, *272*, 91–98.

(14) Chupka, W. A.; Dehmer, P. M.; Jivery, W. T. High resolution photoionization study of ion-pair formation in H_2, HD, and D_2. *J. Chem. Phys.* **1975**, *63*, 3929–3944.

(15) McCulloh, K. E.; Walker, J. A. Photodissociative formation of ion pairs from molecular hydrogen and the electron affinity of the hydrogen atom. *Chem. Phys. Lett.* **1974**, *25*, 439–442.

(16) Pratt, S. T.; McCormack, E. F.; Dehmer, J. L.; Dehmer, P. M. Field-Induced Ion-Pair Formation in Molecular Hydrogen. *Phys. Rev. Lett.* **1992**, *68*, 584–587.

(17) McCormack, E. F.; Pratt, S. T.; Dehmer, P. M.; Dehmer, J. L. Dissociation dynamics of high-v Rydberg states of Molecular Hydrogen. *J. Chem. Phys.* **1993**, *98*, 8370–8383.

(18) Kung, A. H.; Page, R. H.; Larkin, R. J.; Shen, Y. R.; Lee, Y. T. Rydberg Spectroscopy of H_2 via Stepwise Resonant Two-Photon Ion-Pair ($H^+ + H^-$) Production. *Phys. Rev. Lett.* **1986**, *56*, 328–331.

(19) Shiell, R. C.; Hu, X. K.; Hu, Q. C. J.; Hepburn, J. W. Threshold ion-pair production spectroscopy (TIPPS) of H_2 and D_2. *Faraday Discuss.* **2000**, *115*, 331–343.

(20) Reinhold, E.; Ubachs, W. Observation of Coherent Wave Packets in a Heavy Rydberg System. *Phys. Rev. Lett.* **2002**, *88*, 013001.

(21) Reinhold, E.; Ubachs, W. Heavy Rydberg states. *Mol. Phys.* **2005**, *103*, 1329–1352.

(22) Shiell, R. C.; Reinhold, E.; Magnus, F.; Ubachs, W. Control of diabatic *vs.* adiabatic field dissociation in a heavy Rydberg system. *Phys. Rev. Lett.* **2005**, *95*, 213002.

(23) Vieitez, M. O.; Ivanov, T. I.; Reinhold, E.; de Lange, C. A.; Ubachs, W. Observation of a Rydberg series in H^+H^-: A heavy Bohr atom. *Phys. Rev. Lett.* **2008**, *101*, 163001.

(24) Pan, S. H.; Mies, F. H. Rydberg-like properties of rotational vibrational levels and dissociation continuum associated with alkali-halide charge-transfer states. *J. Chem. Phys.* **1988**, *89*, 3096–3103.

(25) Gallagher, T. F. *Rydberg Atoms*; Cambridge University Press: Cambridge, UK, 1994.

(26) Hinnen, P. C. XUV-laser spectroscopy of H_2 and the mystery of the diffuse interstellar bands; PhD Thesis, Vrije Universiteit: Amsterdam 1997.

(27) Reinhold, E.; de Lange, A.; Hogervorst, W.; Ubachs, W. Observation of the $I^1\Pi_g$ outer well state in H_2 and D_2. *J. Chem. Phys.* **1998**, *109*, 9772–9782.

(28) Hinnen, P. C.; Hogervorst, W.; Stolte, S.; Ubachs, W. Sub-Doppler laser spectroscopy of H_2 and D_2 in the range 91−98 nm. *Can. J. Phys.* **1994**, *72*, 1032–1042.

H⁺H⁻ Heavy Rydberg States

J. Phys. Chem. A, Vol. 113, No. 47, 2009 **13245**

(29) Eppink, A. T. J. B.; Parker, D. H. Velocity map imaging of ions and electrons using electrostatic lenses: Application in photoelectron and photofragment ion imaging of molecular oxygen. *Rev. Sci. Instrum.* **1997**, *68*, 3477–3484.

(30) Reinhold, E.; Roeterding, W. G.; Janssen, M. H. M. Ubachs, W. to be published.

(31) Osterwalder, A.; Wuest, A.; Merkt, F.; Jungen, C. High-resolution millimeter wave spectroscopy and multichannel quantum defect theory of the hyperfine structure in high Rydberg states of molecular hydrogen H_2. *J. Chem. Phys.* **2004**, *121*, 11810–11838.

(32) de Lange, A.; Reinhold, E.; Ubachs, W. Precision spectroscopy on some g symmetry states in H_2 and determination of the ionization potential. *Phys. Rev. A* **2002**, *65*, 064501.

(33) Moss, R. E. Calculations for the vibration-rotation levels of H_2^+ in its ground and first excited electronic states. *Mol. Phys.* **1993**, *80*, 1541–1554.

(34) Herzberg, G.; Jungen, Ch. Rydberg Series and ionization potential of the H_2 molecule. *J. Mol. Spectrosc.* **1972**, *41*, 425–486.

(35) Greetham, G.; Hollenstein, U.; Seiler, R.; Ubachs, W.; Merkt, F. High resolution VUV photoionization spectroscopy of HD between the $X^2\Sigma_g^+, v^+ = 0$ and $v^+ = 1$ thresholds. *Phys. Chem. Chem. Phys.* **2003**, *5*, 2528–2534.

(36) Pekeris, C. L. 1^1S, 2^1S, and 2^1S states of H^- and of He. *Phys. Rev. A* **1962**, *126*, 1470–1476.

(37) Asaro, C.; Dalgarno, A. Bound vibrational levels of the 2 lowest $^1\Sigma^+$ states of LiF. *Chem. Phys. Lett.* **1985**, *118*, 64–66.

(38) Safinya, K. A.; Gallagher, T. F. Observation of Interferences between Discrete Autoionizing States in the Photoexcitation Spectrum of Barium. *Phys. Rev. Lett.* **1979**, *43*, 1239–1242.

(39) Jungen, C.; Raoult, M. Spectroscopy in the ionisation continuum. Vibrational preionisation in H_2 calculated by multichannel quantum-defect theory. *Faraday Discuss. Chem. Soc.* **1981**, *71*, 253–271.

(40) Giusti-Suzor, A.; Lefebvre-Brion, H. Theoretical study of complex resonances near ionization thresholds: Application to the N_2 photoionization spectrum. *Phys. Rev. A* **1984**, *30*, 3057–3065.

(41) Müller-Dethlefs, K.; Schlag, E. W. High-resolution zero kinetic energy (ZEKE) photo-electron spectroscopy of molecular systems. *Annu. Rev. Phys. Chem.* **1991**, *42*, 109–136.

(42) Merkt, F.; Zare, R. N. On the lifetimes of Rydberg states probed by delayed pulsed-field ionization. *J. Chem. Phys.* **1994**, *101*, 3495–3505.

(43) Venturelli, L. ATHENA collaboration), Protonium production in ATHENA. *Nucl. Instr. Meth. Phys. Res. B* **2007**, *261*, 40–43.

(44) Rizzini, E. L. First protonium production in a nested Penning trap and related topics. *Can. J. Phys.* **2007**, *85*, 461–467.